



Contents lists available at ScienceDirect

Inorganica Chimica Acta

journal homepage: www.elsevier.com/locate/ica



Research paper

## Increased photocatalytic activity in Ru(II),Rh(III) supramolecular bimetallic complexes with terminal ligand substitution

Hannah J. Sayre<sup>a,\*</sup>, Travis A. White<sup>b</sup>, Karen J. Brewer<sup>a,1</sup><sup>a</sup> Department of Chemistry, Virginia Tech, Blacksburg, VA 24061-0212, USA<sup>b</sup> Department of Chemistry & Biochemistry, The Ohio State University, Columbus, OH 43210-1340, USA

## ARTICLE INFO

## Article history:

Received 16 January 2016

Received in revised form 7 June 2016

Accepted 9 June 2016

Available online xxxxx

## Keywords:

Supramolecular photocatalysis

Water reduction

Electron-withdrawing

Ligand variation

## ABSTRACT

Three new Ru(II),Rh(III) supramolecular bimetallic complexes of the design  $[(\text{Ph}_2\text{phen})_2\text{Ru}(\text{dpp})\text{RhCl}_2(\text{R}_2\text{-bpy})](\text{PF}_6)_3$  ( $\text{R} = \text{CH}_3$  (**Ru-Rh(Me<sub>2</sub>bpy**)),  $\text{H}$  (**Ru-Rh(bpy)**)), or  $\text{COOCH}_3$  (**Ru-Rh(dmeb)**);  $\text{Ph}_2\text{phen} = 4,7$ -diphenyl-1,10-phenanthroline;  $\text{dpp} = 2,3$ -bis(2-pyridyl)pyrazine;  $\text{dmeb} = 4,4'$ -dimethyl ester-2,2'-bipyridine;  $\text{bpy} = 2,2'$ -bipyridine;  $\text{Me}_2\text{bpy} = 4,4'$ -dimethyl-2,2'-bipyridine) have been synthesized and analyzed to determine the impact that the polypyridyl terminal ligand (TL) coordinated to the *cis*-dihalide rhodium(III) metal center has on the photocatalytic activity for water reduction. The bimetallic complexes demonstrate that a correlation exists between the  $\sigma$ -donating ability of the substituted bipyridine ligand, the rate of chloride dissociation upon electrochemical reduction and the activity towards photocatalytic hydrogen production. The weaker  $\sigma$ -donating  $-\text{COOCH}_3$  substituent in **Ru-Rh(dmeb)** increases the rate constant for  $\text{Cl}^-$  dissociation ( $k_{-\text{Cl}} = 0.7 \text{ s}^{-1}$ ) and the amount of  $\text{H}_2$  produced photocatalytically ( $37 \pm 4 \mu\text{mol H}_2$ ,  $63 \pm 7$  turnovers after 20 h; turnovers = mol  $\text{H}_2$ /mol photocatalyst) when compared to  $-\text{H}$  and  $-\text{CH}_3$  substituted complexes **Ru-Rh(bpy)** ( $k_{-\text{Cl}} = 0.2 \text{ s}^{-1}$ ,  $21 \pm 2 \mu\text{mol H}_2$ ,  $35 \pm 3$  turnovers) and **Ru-Rh(Me<sub>2</sub>bpy)** ( $k_{-\text{Cl}} = 0.2 \text{ s}^{-1}$ ,  $18 \pm 2 \mu\text{mol H}_2$ ,  $30 \pm 4$  turnovers), respectively. Varied catalytic activity with respect to the  $\sigma$ -donor capacity of the Rh-TL is attributed to the relative ease of ligand dissociation and the ability to afford rapid electron collection at the Rh metal center.

© 2016 Elsevier B.V. All rights reserved.

## 1. Introduction

The utilization of sunlight to drive thermodynamically demanding reactions that generate alternative fuels (e.g.  $\text{H}_2\text{O}$  splitting to  $\text{H}_2$  and  $\text{O}_2$ ) is an attractive solution to the rise in global energy demands [1–4]. To store solar energy in the form of chemical bonds, light absorbing components harness incident photons that provide the necessary energy and subsequent electrons to reduce  $\text{H}_2\text{O}$  to  $\text{H}_2$  fuel. Significant research efforts have focused on the design of multi-component, homogeneous photocatalytic systems for  $\text{H}_2\text{O}$  reduction that rely on bimolecular, diffusion-based collisions between each component within the photocatalytic system [5–8]. In an effort minimize the number of required bimolecular collisions and to better understand the photocatalytic processes at the molecular level, supramolecular complexes that function as photochemical molecular devices (PMDs) have been developed by covalently coupling the molecular components [9–12].

Photochemical molecular devices that serve to collect multiple reducing equivalents upon photoexcitation are labeled as photoinitiated electron collectors (PECs) and function by collecting electrons in low-lying, unoccupied ligand- or metal-based MOs. Early examples of complexes that collect electrons within the bridging ligand (BL)  $\pi^*$  molecular orbitals include  $\{[(\text{bpy})_2\text{Ru}(\text{dpp})]_2\text{IrCl}_2\}^{5+}$  ( $\text{dpp} = 2,3$ -bis(2-pyridyl)benzoquinoline) and  $\{(\text{phen})_2\text{Ru}(\text{BL})\text{Ru}(\text{phen})_2\}^{4+}$  ( $\text{phen} = 1,10$ -phenanthroline;  $\text{BL} = \text{tatpp} = 9,11,20,22$ -tetraazatetrapyrido[3,2-*a*:2',3'-*c*:3'',2''-1:2''',3''''-*n*]pentacene;  $\text{tatpq} = 9,11,20,22$ -tetraazatetrapyrido[3,2-*a*:2',3'-*c*:3'',2''-1:2''',3''''-*n*]pentacene-10,21-quinone), yet these systems do not serve as photocatalysts for  $\text{H}_2\text{O}$  reduction [12–14]. Modification of the BL and reactive metal (RM) of  $\{[(\text{bpy})_2\text{Ru}(\text{dpp})]_2\text{IrCl}_2\}^{5+}$  to form  $\{[(\text{bpy})_2\text{Ru}(\text{dpp})]_2\text{RhCl}_2\}^{5+}$  ( $\text{dpp} = 2,3$ -bis(2-pyridyl)pyrazine) generated the first PMD for PEC at a metal site to function as a photocatalyst for  $\text{H}_2\text{O}$  reduction [15,16]. In the presence of the sacrificial electron donor *N,N*-dimethylaniline (DMA) and light, the  $\{[(\text{bpy})_2\text{Ru}(\text{dpp})]_2\text{RhCl}_2\}^{5+}$  trimetallic complex functions via successive photoexcitations of the Ru-based LA to transfer electrons to the *cis*- $\text{Rh}^{\text{III}}\text{Cl}_2$  site which dissociates two halide ligands and generates a coordinatively unsaturated, four coordinated  $\text{Rh}^{\text{I}}$  species,  $\{[(\text{bpy})_2\text{Ru}(\text{dpp})]_2\text{Rh}^{\text{I}}\}^{5+}$ , that is capable of  $\text{H}_2\text{O}$  reduction to  $\text{H}_2$ .

\* Corresponding author at: Department of Chemistry & Biochemistry, The Ohio State University, Columbus, OH 43210-1340, USA.

E-mail address: sayre.166@osu.edu (H.J. Sayre).

<sup>1</sup> Deceased October 24, 2014.

Structural and component modifications of systems that couple LA subunits to a RM center through a polypyridyl BL have resulted in an array of photocatalytically-active architectures for H<sub>2</sub>O reduction to H<sub>2</sub> [17–23]. Within the Ru(II),Rh(III),Ru(II) trimetallic architecture  $[(\text{TL})_2\text{Ru}(\text{dpp})_2\text{RhX}_2]^{3+}$  (TL = bpy, phen, Ph<sub>2</sub>phen; X = Cl<sup>-</sup>, Br<sup>-</sup>, OH<sup>-</sup>), bidentate and monodentate ligand variation has produced a library of complexes with varied electrochemical and photophysical properties and photocatalytic H<sub>2</sub>O reduction activity [24–28]. The light absorbing and excited state properties of the Ru-based LA subunit are strongly impacted by the choice of polypyridyl TL, while the catalytic activity at the Rh-based RM center is tuned by monodentate X identity. The trimetallic complex  $[(\text{Ph}_2\text{phen})_2\text{Ru}(\text{dpp})_2\text{RhBr}_2]^{3+}$  is a highly active H<sub>2</sub>O reduction photocatalyst when compared with the  $[(\text{phen})_2\text{Ru}(\text{dpp})_2\text{RhBr}_2]^{3+}$  trimetallic analogue, producing 1640 vs. 180 μmol H<sub>2</sub>, respectively, after 20 h photolysis in a *N,N*-dimethylformamide (DMF) solution containing DMA electron donor [27]. This minor change to the polypyridyl TL structure significantly enhances photocatalytic activity and thereby emphasizes the importance of design considerations when developing new H<sub>2</sub>O reduction photocatalysts.

Substitution of one LA subunit with a polypyridyl TL in the Ru(II),Rh(III),Ru(II) trimetallic architecture has produced Ru(II),Rh(III) bimetallic complexes of the general formula  $[(\text{TL})_2\text{Ru}(\text{BL})\text{RhX}_2(\text{TL}')]^{3+}$  in an effort to better understand the role and necessity of the second LA subunit [29]. The judicious choice of molecular components throughout the Ru(II),Rh(III) bimetallic architecture dictates photocatalytic activity towards H<sub>2</sub>O reduction through a careful balance of sterics, electronics, light absorption, and ion pairing throughout the photocatalytic cycle [30–34]. The bimetallic complexes  $[(\text{Ph}_2\text{phen})_2\text{Ru}(\text{dpp})\text{RhX}_2(\text{Ph}_2\text{phen})]^{3+}$  (X = Cl<sup>-</sup> or Br<sup>-</sup>) represent a systematic study undertaken to determine the influence that the σ-donating ability and degree of ion pairing imparted by the monodentate halide ligands have on the photocatalytic H<sub>2</sub>O reduction activity [30]. Previous reports that vary the electronic character (σ-donor/π-acceptor) of the bidentate polypyridyl ligand coordinated to Rh within a monometallic complex,  $[\text{Rh}(\text{R}_2\text{-bpy})_2\text{Cl}_2]^+$  (R = H or C(CH<sub>3</sub>)<sub>3</sub>) [35] and  $[\text{Rh}(\text{BL})_2\text{Br}_2]^+$  (BL = dpp, dpq, or dpb) [36], display how differences in electron density at the Rh metal center can impact the observed catalysis. Conversely, a systematic study to decipher the electronic contributions at the Rh site *via* variation of the polypyridyl TL's σ-donating ability has yet to be reported for the  $[(\text{TL})_2\text{Ru}(\text{BL})\text{RhX}_2(\text{TL}')]^{3+}$  bimetallic architecture and necessitates such analysis.

Herein we report the synthesis, characterization, and photocatalytic activity of a series of Ru(II),Rh(III) bimetallic complexes of the design  $[(\text{Ph}_2\text{phen})_2\text{Ru}(\text{dpp})\text{RhCl}_2(\text{R}_2\text{-bpy})]^{3+}$  (R = CH<sub>3</sub> (**Ru-Rh(Me<sub>2</sub>bpy)**)), H (**Ru-Rh(bpy)**), or COOCH<sub>3</sub> (**Ru-Rh(dmeb)**); Fig. 1) to investigate what impact electronic variation of the Rh-TL σ-donating ability will have on the observed photocatalytic reduction of H<sub>2</sub>O to H<sub>2</sub>. The Ru-based LA subunit, (Ph<sub>2</sub>phen)<sub>2</sub>Ru<sup>II</sup>(dpp), is not altered in an effort to minimize any contributions that the light absorber component would have on the Rh-TL electronic comparisons. The pK<sub>a</sub> values for similarly substituted pyridinium compounds (4-methoxycarbonylpyridinium = 3.26; pyridinium = 5.23; 4-methylpyridinium = 5.97) [37] can provide an approximation for the σ-bonding character of the polypyridyl TL (σ-donor ability: Me<sub>2</sub>bpy ~ bpy > dmeb). Inclusion of stronger (-CH<sub>3</sub>) vs. weaker (-COOCH<sub>3</sub>) σ-type electron-donating substituents on 2,2'-bipyridine modulates electron density on the Rh center and not only impacts the rate constant for halide dissociation upon electrochemical reduction (*k*<sub>-Cl</sub>: **Ru-Rh(dmeb)** > **Ru-Rh(Me<sub>2</sub>bpy)** ~ **Ru-Rh(bpy)**), but also the ability to catalyze H<sub>2</sub>O reduction (μmol of H<sub>2</sub>: **Ru-Rh(dmeb)** > **Ru-Rh(Me<sub>2</sub>bpy)** ~ **Ru-Rh(bpy)**).

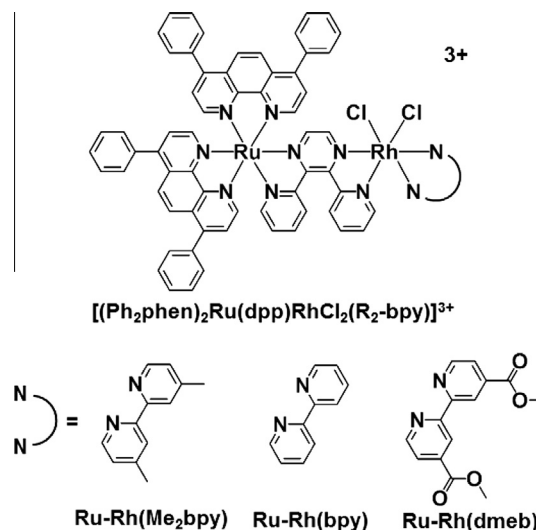


Fig. 1. Structural representation of  $[(\text{Ph}_2\text{phen})_2\text{Ru}(\text{dpp})\text{RhCl}_2(\text{R}_2\text{-bpy})](\text{PF}_6)_3$  complexes (R = CH<sub>3</sub>, H, or COOCH<sub>3</sub>).

## 2. Experimental

### 2.1. Materials and methods

All materials for syntheses and characterizations were used as received unless otherwise stated. RuCl<sub>3</sub>·xH<sub>2</sub>O, RhCl<sub>3</sub>·xH<sub>2</sub>O, 4,7-diphenyl-1,10-phenanthroline (Ph<sub>2</sub>phen), 2,3-bis(2-pyridyl)pyrazine (dpp), 2,2'-bipyridine (bpy), and Sephadex® LH-20 resin were purchased from Aldrich. 4,4'-Dimethyl-2,2'-bipyridine (Me<sub>2</sub>bpy) was purchased from Atomax Chemicals. Neutral, activated alumina was purchased from Alfa Aesar and deactivated using methanol. Spectrophotometric grade acetonitrile was purchased from Spectrum Chemicals. 4,4'-Dimethyl ester-2,2'-bipyridine (dmeb) [38],  $[(\text{Ph}_2\text{phen})_2\text{RuCl}_2]$  [39],  $[(\text{Ph}_2\text{phen})_2\text{Ru}(\text{dpp})](\text{PF}_6)_2$  [40] and  $[\text{Rh}(\text{bpy})\text{Cl}_3(\text{MeOH})](\text{MeOH})$  [41] were synthesized as previously reported.

### 2.2. Syntheses

#### 2.2.1. $[\text{Rh}(\text{Me}_2\text{bpy})\text{Cl}_3(\text{DMF})]$

The new Rh monometallic complex was synthesized using a similar procedure reported for  $[\text{Rh}(\text{bpy})\text{Cl}_3(\text{DMF})]$  (DMF = *N,N*-dimethylformamide) [34]. RhCl<sub>3</sub>·xH<sub>2</sub>O (0.20 g, 0.75 mmol) and 4,4'-dimethyl-2,2'-bipyridine (0.017 g, 0.92 mmol) were heated at 60 °C in 2 mL DMF for 2 h with rapid stirring. The resultant orange-yellow solution was allowed to cool to room temperature and was added dropwise to stirring diethyl ether to induce precipitation. The orange precipitate was collected by vacuum filtration, dissolved in chloroform, and filtered into a clean flask. The solvent was removed from the yellow filtrate by rotary evaporation to produce a yellow solid (yield = 67%, 0.24 g, 0.51 mmol). ESI-MS:  $[\text{M}-\text{Cl}^-]^+ m/z = 430.85$ .

#### 2.2.2. $[\text{Rh}(\text{dmeb})\text{Cl}_3(\text{DMF})]$

The new Rh monometallic complex was synthesized as described above using RhCl<sub>3</sub>·xH<sub>2</sub>O (0.20 g, 0.76 mmol) and 4,4'-dimethyl ester-2,2'-bipyridine (0.26 g, 0.92 mmol). Yield = 79%, 0.34 g, 0.61 mmol. ESI-MS:  $[\text{M}+\text{NH}_4^+]^+ m/z = 570.98$ .

#### 2.2.3. $[(\text{Ph}_2\text{phen})_2\text{Ru}(\text{dpp})\text{RhCl}_2(\text{Me}_2\text{bpy})](\text{PF}_6)_3$ (**Ru-Rh(Me<sub>2</sub>bpy)**)

The new Ru(II),Rh(III) bimetallic complex was synthesized using a similar procedure reported for  $[(\text{bpy})_2\text{Ru}(\text{dpp})\text{RhCl}_2$

(phen)](PF<sub>6</sub>)<sub>3</sub> [29]. [(Ph<sub>2</sub>phen)<sub>2</sub>Ru(dpp)](PF<sub>6</sub>)<sub>2</sub> (0.48 g, 0.37 mmol) and [Rh(Me<sub>2</sub>bpy)Cl<sub>3</sub>(DMF)] (0.24 g, 0.51 mmol) were heated at reflux in 30 mL 2:1 ethanol/water (v/v) for 3 h with rapid stirring. The dark red solution was cooled to room temperature and precipitated in aqueous NH<sub>4</sub>PF<sub>6</sub>. The dark red precipitate was collected by vacuum filtration and rinsed with water and diethyl ether. The crude product was purified using size exclusion chromatography with Sephadex<sup>®</sup> LH-20 resin as the stationary phase and a 2:1 ethanol/acetonitrile (v/v) solvent mixture as the mobile phase. Multiple fractions were collected and analyzed by electronic absorption and emission spectroscopies to ensure the absence of the emissive [(Ph<sub>2</sub>phen)Ru(dpp)](PF<sub>6</sub>)<sub>2</sub> monometallic ( $\lambda_{em}$  = 680 nm) when excited at  $\lambda_{abs}$  = 520 nm. Fractions which did not emit at 680 nm were combined and the solvent removed by rotary evaporation. The product was dissolved in minimal acetonitrile and added to stirring ether to induce precipitation. The precipitate was collected by vacuum filtration and dried in air to produce a dark red solid (yield = 15%, 0.10 g, 0.074 mmol). ESI-MS: [M–PF<sub>6</sub>]<sup>+</sup> *m/z* = 1647.12.

#### 2.2.4. [(Ph<sub>2</sub>phen)<sub>2</sub>Ru(dpp)RhCl<sub>2</sub>(dmeb)](PF<sub>6</sub>)<sub>3</sub> (**Ru-Rh(dmeb)**)

The new Ru(II),Rh(III) bimetallic complex was synthesized as described above using [(Ph<sub>2</sub>phen)<sub>2</sub>Ru(dpp)](PF<sub>6</sub>)<sub>2</sub> (0.48 g, 0.37 mmol) and [Rh(dmeb)Cl<sub>3</sub>(DMF)] (0.29 g, 0.51 mmol). Yield = 18%, 0.12 g, 0.083 mmol. ESI-MS: [M–PF<sub>6</sub>]<sup>+</sup> *m/z* = 1735.10.

#### 2.2.5. [(Ph<sub>2</sub>phen)<sub>2</sub>Ru(dpp)RhCl<sub>2</sub>(bpy)](PF<sub>6</sub>)<sub>3</sub> (**Ru-Rh(bpy)**)

The new Ru(II),Rh(III) bimetallic complex was synthesized as described above using [(Ph<sub>2</sub>phen)<sub>2</sub>Ru(dpp)](PF<sub>6</sub>)<sub>2</sub> (0.47 g, 0.37 mmol) and [Rh(bpy)Cl<sub>3</sub>(MeOH)](MeOH) (0.21, 0.50 mmol). Yield = 35%, 0.23 g, 0.17 mmol. ESI-MS: [M–PF<sub>6</sub>]<sup>+</sup> *m/z* = 1619.10.

### 2.3. Physical measurements

Cyclic voltammograms (CV) were performed at room temperature using a BAS Epsilon potentiostat with a glassy carbon disk working electrode, platinum wire auxiliary electrode and Ag/AgCl reference electrode (3 M NaCl) in 0.1 M <sup>n</sup>Bu<sub>4</sub>NPF<sub>6</sub>/CH<sub>3</sub>CN electrolyte. Solutions were purged with argon prior to measurement and blanketed with argon during CV scans. The rate constants for halide dissociation (*k*<sub>–Cl</sub>) were determined by comparing experimental voltammograms with those of simulated voltammograms using BASi DigiSim<sup>®</sup> version 3.0 simulation software for cyclic voltammetry [42,43]. Simulated voltammograms were fit using the formulae for quasi-reversible couples that possess an electron transfer step (E) followed by a chemical reaction step (C) as shown in Eqs. (1) and (2), respectively.



Other pertinent parameters included  $\nu$  = 100 and 1000 mV/s, resistance = 100–300 ohms, T = 298 K,  $E^0$  = –0.38 V for **Ru-Rh(dmeb)** and  $E^0$  = –0.41 V for **Ru-Rh(Me<sub>2</sub>bpy)** and **Ru-Rh(bpy)**,  $\alpha$  /  $\lambda$  = 0.5 eV and  $K_{eq}$  =  $1 \times 10^{10}$ .

A Hewlett-Packard 8452A diode array spectrophotometer was employed for electronic absorption spectroscopy and spectra were collected in spectrophotometric grade CH<sub>3</sub>CN using a 1 cm quartz cuvette (Starna Cells; Atascadero, CA). Extinction coefficient values were measured in triplicate. Steady-state luminescence spectroscopy was performed with a water-cooled 150 W xenon arc lamp with a 540 nm excitation using a Quanta Master Model QA-200-45E fluorimeter from Photon Technologies International and a thermo-electric cooled Hamamatsu R2658 photomultiplier tube. Time-resolved luminescence spectroscopy was carried out with an Edinburgh Instruments FLS920 time-correlated single photon

counter with a 508.6 nm excitation wavelength and monitoring 790 nm emission.

Photocatalytic hydrogen production experiments were performed similar to a previously reported method [30]. The photolysis setup consisted of a locally designed LED array [44] and H<sub>2</sub>scan HY-OPTIMA 700 hydrogen sensors (Valencia, CA) to permit real time monitoring of hydrogen evolution. Empty, air-tight photolysis reaction cells were connected to hydrogen sensors and deoxygenated using argon gas. Stock catalyst solutions prepared in DMF were combined with acidified deionized water (pH = 2 with CF<sub>3</sub>SO<sub>3</sub>H) in the air-tight photolysis cells and were further deoxygenated. The *N,N*-dimethylaniline (DMA) electron donor was purged separately with argon gas and injected into the catalyst solutions immediately prior to photolysis. The total solution volume was 4.5 mL, consisting of 130  $\mu$ M catalyst, 1.5 M DMA, 0.62 M H<sub>2</sub>O and 0.11 mM [DMAH<sup>+</sup>][CF<sub>3</sub>SO<sub>3</sub><sup>–</sup>] with a 15.5 mL headspace. The solutions were photolyzed with 470 nm light (light flux =  $2.36 \pm 0.05 \times 10^{19}$  photons/min). The reported value for H<sub>2</sub> production is the average of three experiments.

## 3. Results and discussion

### 3.1. Synthesis

The title Ru(II),Rh(III) bimetallic complexes were synthesized using a building block approach outlined in Fig. 2. The [(Ph<sub>2</sub>phen)<sub>2</sub>RuCl<sub>2</sub>] starting material was prepared by reacting two equivalents of the Ph<sub>2</sub>phen terminal ligand with RuCl<sub>3</sub>·xH<sub>2</sub>O, followed by alumina column chromatography to remove the highly emissive [Ru(Ph<sub>2</sub>phen)<sub>3</sub>]<sup>2+</sup> impurity. The [(Ph<sub>2</sub>phen)<sub>2</sub>Ru(dpp)]<sup>+</sup> light absorber subunit was prepared by substituting the labile Cl<sup>–</sup> ligands with the bis-bidentate dpp BL. Separately, the [Rh(R<sub>2</sub>-bpy)Cl<sub>3</sub>(DMF)]<sup>+</sup> monometallic complexes were synthesized by gently heating a solution of RhCl<sub>3</sub>·xH<sub>2</sub>O and one equivalent of the bidentate TL in DMF, followed by precipitation with diethyl ether and rinsing with H<sub>2</sub>O to remove unreacted RhCl<sub>3</sub>·xH<sub>2</sub>O starting material. The Ru(II) and Rh(III) monometallic precursors were heated at reflux in 2:1 (v/v) EtOH/H<sub>2</sub>O solution and purified using size-exclusion chromatography to produce the new bimetallic complexes **Ru-Rh(Me<sub>2</sub>bpy)**, **Ru-Rh(bpy)**, and **Ru-Rh(dmeb)**. The Ru(II),Rh(III) bimetallic complexes were characterized using ESI-MS, electrochemical analysis, and steady-state and time-resolved spectroscopic techniques.

### 3.2. Electrochemistry

Electrochemistry provides information pertaining to the frontier molecular orbital energies and the subsequent chemical reactivity following heterogeneous electron transfer [45]. Cyclic voltammograms (CVs) of the title Ru(II),Rh(III) complexes (Fig. 3) display similar redox-activity and features as those for previously reported polyazine-bridged Ru(II),Rh(III) bimetallic complexes that possess a *cis*-Rh<sup>III</sup>X<sub>2</sub> center [29–33,46]. Anodic scans display a reversible, one-electron Ru<sup>II/III</sup> oxidation at  $E_{1/2}$  = +1.60 V vs. Ag/AgCl for all three bimetallic complexes, indicative of minimal-to-negligible electronic communication between the Ru(II) metal center and the terminal ligand coordinated to Rh(III). Similarly, Ru<sup>II/III</sup> oxidation of the previously reported [(Ph<sub>2</sub>phen)<sub>2</sub>Ru(dpp)RhX<sub>2</sub>(Ph<sub>2</sub>phen)]<sup>3+</sup> (X = Cl<sup>–</sup> or Br<sup>–</sup>) bimetallic complexes occurs at  $E_{1/2}$  = +1.59 V vs. Ag/AgCl, providing further evidence of electronic isolation between Ru(II) and Rh-TL [30].

Cathodic scans present somewhat complicated electrochemistry given the nearly isoenergetic nature of the dpp( $\pi^*$ ) and Rh( $d\sigma^*$ ) unoccupied MOs and the competitive electrochemical mechanisms upon reduction [32]. The bimetallic complexes display a reversible reduction at –0.41 V vs. Ag/AgCl for **Ru-Rh(Me<sub>2</sub>bpy)**

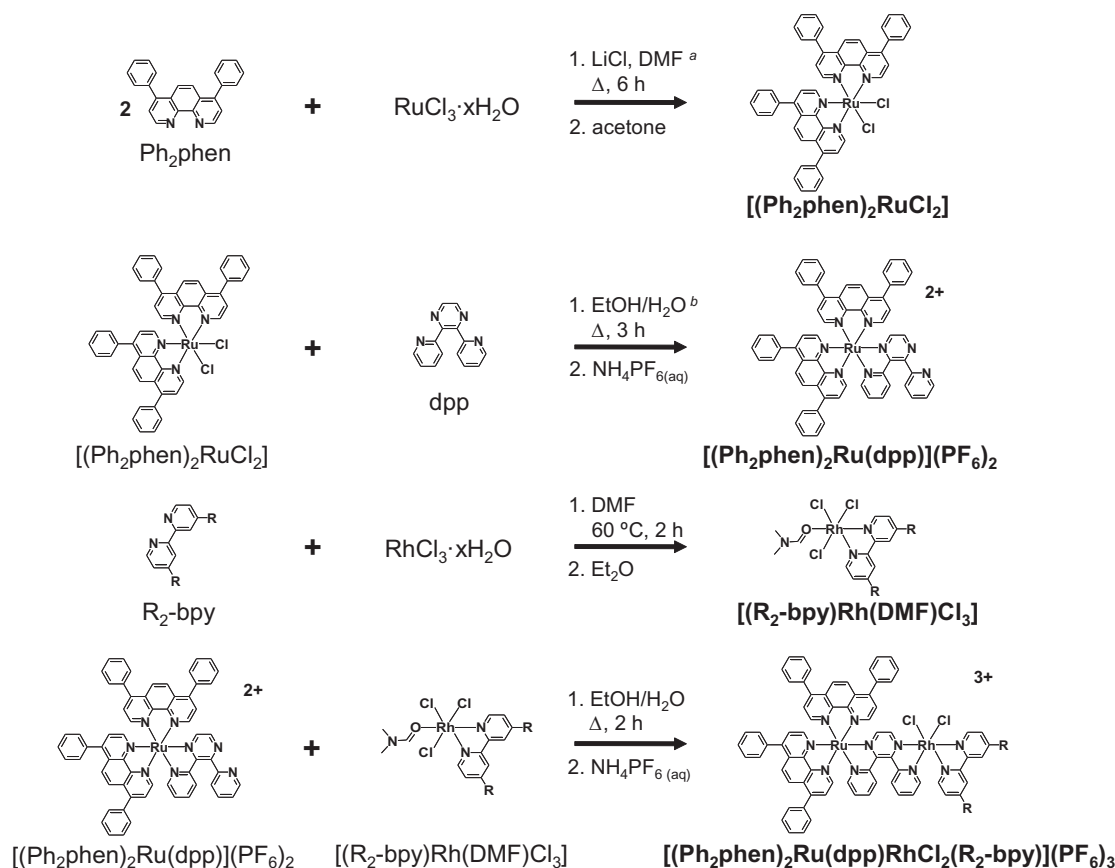


**Fig. 2.** General building block synthetic approach for the preparation of **Ru-Rh(Me<sub>2</sub>bpy)**, **Ru-Rh(bpy)**, **Ru-Rh(dmeb)** bimetallic complexes (see Section 2 for details). <sup>a</sup>Reference [39]. <sup>b</sup>Reference [40].

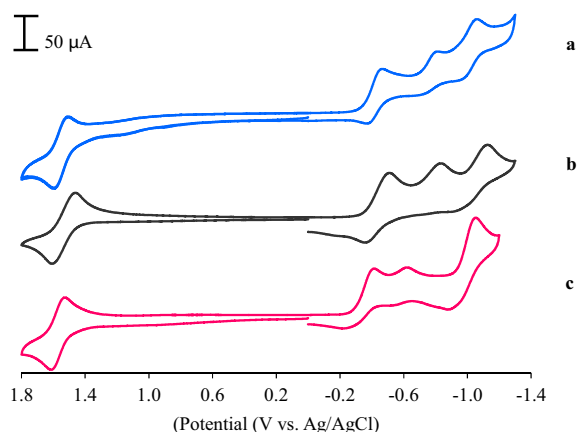


**Fig. 3.** Cyclic voltammograms of **Ru-Rh(Me<sub>2</sub>bpy)** (a), **Ru-Rh(bpy)** (b) and **Ru-Rh(dmeb)** (c) measured at RT under Ar atm in 0.1 M <sup>n</sup>Bu<sub>4</sub>NPF<sub>6</sub> supporting electrolyte in CH<sub>3</sub>CN solvent at a scan rate of 100 mV/s.

and **Ru-Rh(bpy)** and a quasi-reversible reduction at  $-0.38$  V vs. Ag/AgCl for **Ru-Rh(dmeb)** (Fig. 3). This first cathodic couple is labeled as an ECEC process consisting of a Rh<sup>III</sup>/Cl<sub>2</sub> reduction followed by chloride dissociation and subsequent Rh<sup>III</sup>/Cl reduction prior to cleavage of the second Rh–Cl bond [32]. Varied reversibility of the first cathodic couple is attributed to differing rates of chloride dissociation following the first reduction. The rate constant for chloride dissociation ( $k_{-Cl}$ ) was further investigated using DigiSim<sup>®</sup> to model the first reductive couple with an EC mechanism from Eqs. (1) and (2) (Fig. 4). Simulations provide an esti-

ated  $k_{-Cl}$  value of  $0.2 \text{ s}^{-1}$  for **Ru-Rh(Me<sub>2</sub>bpy)** and **Ru-Rh(bpy)** and  $0.7 \text{ s}^{-1}$  for **Ru-Rh(dmeb)**. The second cathodic couple is labeled an EECC process whereby a portion of the one-electron reduced species, Rh<sup>II</sup>Cl<sub>2</sub>, does not dissociate chloride rapidly and undergoes further reduction prior to dissociation of both chloride ligands [32]. The second cathodic couple shifts from  $E_p^c = -0.82$  V vs. Ag/AgCl for **Ru-Rh(Me<sub>2</sub>bpy)** and  $E_p^c = -0.80$  V vs. Ag/AgCl for **Ru-Rh(bpy)** to  $E_p^c = -0.68$  V vs. Ag/AgCl for **Ru-Rh(dmeb)** which supports more rapid chloride dissociation with the methyl ester-substituted TL. The faster rate of chloride dissociation following reduction for **Ru-Rh(dmeb)** suggests increased formation of a coordinatively-unsaturated Rh metal center for potential catalysis, an important factor in the generation of a highly active catalyst. Importantly, the frontier molecular orbitals within this Ru(II),Rh(III) architecture are described as primarily Ru(II) HOMO and Rh(III) LUMO in character.

### 3.3. Electronic absorption spectroscopy

The light absorbing ability of the Ru(II),Rh(III) bimetallic complexes was measured using electronic absorption spectroscopy and are tabulated in Table 1. As observed with similar complexes [29–31,33,46], **Ru-Rh(Me<sub>2</sub>bpy)**, **Ru-Rh(bpy)** and **Ru-Rh(dmeb)** are strong light absorbers throughout the UV and visible with polypyridyl  $\pi \rightarrow \pi^*$  intraligand (<sup>1</sup>IL) transitions in the UV and Ru( $d\pi$ )  $\rightarrow$  ligand( $\pi^*$ ) metal-to-ligand charge transfer (<sup>1</sup>MLCT) transitions in the visible (Fig. 5). For all three bimetallic complexes, the lowest energy transition is ascribed to the Ru( $d\pi$ )  $\rightarrow$   $\mu$ -dpp( $\pi^*$ ) <sup>1</sup>MLCT transition at  $\lambda_{max} = 512$  nm for **Ru-Rh(Me<sub>2</sub>bpy)** and **Ru-Rh(bpy)** and at  $\lambda_{max} = 520$  nm for **Ru-Rh(dmeb)**. The small <sup>1</sup>MLCT

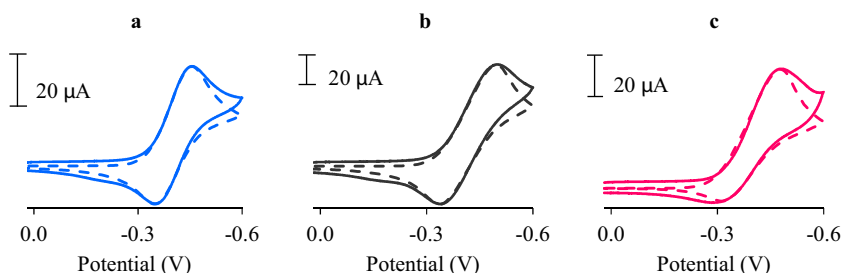


**Fig. 4.** Experimental CVs of the first cathodic couple (solid line) and simulated CVs using DigiSim® (dashed line) of **Ru-Rh(Me<sub>2</sub>bpy)** (a), **Ru-Rh(bpy)** (b) and **Ru-Rh(dmeb)** (c) with a scan rate of 100 mV/s in 0.1 M <sup>t</sup>Bu<sub>4</sub>NPF<sub>6</sub>/CH<sub>3</sub>CN.

**Table 1**  
Light absorbing properties of Ru(II),Rh(III) bimetallic complexes.

Complex <sup>a</sup>	λ <sup>abs</sup> (nm)	ε × 10 <sup>-4</sup> (M <sup>-1</sup> cm <sup>-1</sup> )	Assignment
<b>Ru-Rh(Me<sub>2</sub>bpy)</b>	278	10.2	Ph <sub>2</sub> phen π → π*
	426	1.9	Ru(dπ) → Ph <sub>2</sub> phen(π*) <sup>1</sup> CT
	512	2.0	Ru(dπ) → μ-dpp(π*) <sup>1</sup> CT
<b>Ru-Rh(bpy)</b>	278	10.2	Ph <sub>2</sub> phen π → π*
	426	1.9	Ru(dπ) → Ph <sub>2</sub> phen(π*) <sup>1</sup> CT
	512	1.9	Ru(dπ) → μ-dpp(π*) <sup>1</sup> CT
<b>Ru-Rh(dmeb)</b>	278	10.2	Ph <sub>2</sub> phen π → π*
	426	1.9	Ru(dπ) → Ph <sub>2</sub> phen(π*) <sup>1</sup> CT
	520	1.8	Ru(dπ) → μ-dpp(π*) <sup>1</sup> CT
<b>Ru-Rh(Ph<sub>2</sub>phen)</b> <sup>b</sup>	278	10.7	Ph <sub>2</sub> phen π → π*
	414	1.7	Ru(dπ) → Ph <sub>2</sub> phen(π*) <sup>1</sup> CT
	514	1.6	Ru(dπ) → μ-dpp(π*) <sup>1</sup> CT

<sup>a</sup> Measured at RT in spectrophotometric grade CH<sub>3</sub>CN using a 1 cm quartz cuvette.

<sup>b</sup> Values reported from reference [30]; **Ru-Rh(Ph<sub>2</sub>phen)** corresponds to [(Ph<sub>2</sub>phen)<sub>2</sub>Ru(dpp)RhCl<sub>2</sub>(Ph<sub>2</sub>phen)]<sup>3+</sup>.

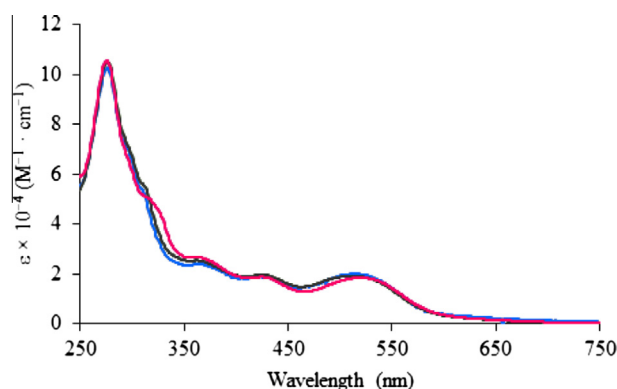


**Fig. 5.** Electronic absorption of **Ru-Rh(Me<sub>2</sub>bpy)** (blue), **Ru-Rh(bpy)** (black) and **Ru-Rh(dmeb)** (red) measured in CH<sub>3</sub>CN at RT. (For interpretation of the references to colour in this figure legend, the reader is referred to the web version of this article.)

energy difference throughout the series of [(Ph<sub>2</sub>phen)<sub>2</sub>Ru(dpp)RhCl<sub>2</sub>(TL)]<sup>3+</sup> complexes (λ<sub>max</sub> = 514 nm for TL = Ph<sub>2</sub>phen [30]) is not surprising given the same (Ph<sub>2</sub>phen)<sub>2</sub>Ru(dpp) LA subunit dominates the UV–vis spectrum, as well as possessing a RhCl<sub>2</sub>(TL) RM subunit. Modification of the Rh-TL does not strongly alter the [(Ph<sub>2</sub>phen)<sub>2</sub>Ru(dpp)RhCl<sub>2</sub>(TL)]<sup>3+</sup> complexes' light absorbing ability and maintains the Ru(dπ) → μ-dpp(π\*)<sup>1</sup>MLCT as the lowest energy transition to direct electron density towards the RhCl<sub>2</sub>(TL) RM subunit upon photoexcitation.

### 3.4. Emission spectroscopy

Steady-state and time-resolved emission spectroscopies provide insight into the excited state dynamics of the title Ru(II),Rh(III) bimetallic complexes and these properties are summarized in Table 2. A simplified Jablonski diagram is shown in Fig. 6 to provide an overview of possible excited state deactivation processes. Upon visible light photoexcitation, population of the Ru(dπ) → μ-dpp(π\*)<sup>1</sup>MLCT excited state (ES) is followed by intersystem crossing to populate the weakly emissive Ru(dπ) → μ-dpp(π\*)<sup>3</sup>MLCT ES. The <sup>3</sup>MLCT emission energy (λ<sup>em</sup>), emission quantum yield (Φ<sup>em</sup>), and ES lifetime (τ<sup>em</sup>) are similar for all three Ru(II),Rh(III) bimetallic complexes, indicating that minimal electronic perturbations are imparted on the ES dynamics upon Rh-TL variation. Weak emission from the <sup>3</sup>MLCT ES is due to low-lying, unoccupied Rh(dσ\*) MOs which permit facile intramolecular electron transfer to populate a non-emissive Ru(dπ) → Rh(dσ\*)<sup>3</sup>MMCT (metal-to-metal charge transfer) ES. The rate constant for intramolecular electron transfer (*k<sub>et</sub>*) was calculated (Eqs. (3)–(5)) using the homobimetallic model complex, [(Ph<sub>2</sub>phen)<sub>2</sub>Ru]<sub>2</sub>(dpp)]<sup>4+</sup> (labeled **(Ph<sub>2</sub>phen)<sub>2</sub>Ru-Ru**), which also emits from a Ru(dπ) → μ-dpp(π\*)<sup>3</sup>MLCT but does not possess a <sup>3</sup>MMCT ES. The rate constants for <sup>3</sup>MLCT ES radiative (*k<sub>r</sub>*) and non-radiative (*k<sub>nr</sub>*) decay of the **(Ph<sub>2</sub>phen)<sub>2</sub>Ru-Ru** model complex are used as an estimate for the Ru(II),Rh(III) bimetallic complexes given the similar ES manifold [47].

$$\tau_{Ru,Rh} = \frac{1}{k_r + k_{nr} + k_{et}} \quad (3)$$

$$\tau_{Ru,Ru} = \frac{1}{k_r + k_{nr}} \quad (4)$$

$$k_{et} = \frac{1}{\tau_{Ru,Rh}} - \frac{1}{\tau_{Ru,Ru}} \quad (5)$$

As shown in Table 2, the *k<sub>et</sub>* values for the title Ru(II),Rh(III) bimetallic complexes are similar and further imply that efficient population of the <sup>3</sup>MMCT ES occurs regardless of Rh-TL identity. Equally important is the large order of magnitude (10<sup>7</sup> s<sup>-1</sup>) calculated for intramolecular electron transfer that produces a formally oxidized Ru(III) and formally reduced Rh(II) species in the absence of a sacrificial quencher species such as *N,N*-dimethylaniline (DMA). Rapid, directional charge separation is vital to the formation of photochemically-active excited states towards the photocatalytic reduction of H<sub>2</sub>O to H<sub>2</sub>.

### 3.5. Photocatalysis studies

Photocatalytic H<sub>2</sub>O reduction experiments were performed in an effort to elucidate the impact of Rh-TL identity within the Ru(II),Rh(III) bimetallic architecture. The new bimetallic complexes **Ru-Rh(Me<sub>2</sub>bpy)**, **Ru-Rh(bpy)**, and **Ru-Rh(dmeb)** are active photo-

**Table 2**  
Excited state properties of Ru(II),Rh(III) bimetallic complexes.

Complex <sup>a</sup>	$\lambda^{em}$ (nm)	$\Phi^{em}$ (10 <sup>-4</sup> )	$\tau^{em}$ (ns)	$k_r$ (10 <sup>4</sup> s <sup>-1</sup> )	$k_{nr}$ (10 <sup>6</sup> s <sup>-1</sup> )	$k_{et}$ (10 <sup>7</sup> s <sup>-1</sup> )
<b>Ru-Rh</b> ( <b>Me<sub>2</sub>bpy</b> )	808	5.2	20	1.0	5.9	4.4
<b>Ru-Rh(bpy)</b>	808	4.7	19	1.0	5.9	4.7
<b>Ru-Rh(dmeb)</b>	787	6.4	19	1.0	5.9	4.8
<b>(Ph<sub>2</sub>phen)<sub>2</sub>Ru-Ru<sup>b</sup></b>	754	17.3	170	1.0	5.9	–

<sup>a</sup> Measured at RT in Ar-deoxygenated, spectrophotometric grade CH<sub>3</sub>CN using a 1 cm quartz cuvette.

<sup>b</sup> Values reported from reference [48]; **(Ph<sub>2</sub>phen)<sub>2</sub>Ru-Ru** corresponds to  $[(Ph_2phen)_2Ru_2(dpp)]^{4+}$ .

catalysts for H<sub>2</sub> production when excited with 470 nm light in DMF solvent in the presence of H<sub>2</sub>O substrate and DMA electron donor, Fig. 7. Although the light absorbing and excited state properties of the modified Rh-TL complexes are similar, the photocatalytic activity displays a large disparity between the **Ru-Rh(dmeb)** complex (37 ± 4 μmol H<sub>2</sub>, 63 ± 7 TON after 20 h) and the **Ru-Rh(Me<sub>2</sub>bpy)** and **Ru-Rh(bpy)** complexes (18 ± 2 μmol H<sub>2</sub>, 30 ± 4 TON; 21 ± 2 μmol H<sub>2</sub>, 35 ± 3 TON, respectively) (Table 3). Maximum quantum yields for H<sub>2</sub> evolution after 4 h photolysis (Max. Φ) with **Ru-Rh(Me<sub>2</sub>bpy)**, **Ru-Rh(bpy)** and **Ru-Rh(dmeb)** are 0.002, 0.003 and 0.004, respectively. Recent reports by our group [30] and Rau and co-workers [18] have demonstrated that the halide ligand coordinated to the reactive metal center, RhCl<sub>2</sub> vs. RhBr<sub>2</sub> in the former and PtCl<sub>2</sub> vs. PtI<sub>2</sub> in the latter, dictates photocatalytic activity towards H<sub>2</sub> production regardless of the similar photophysical properties within each series. The weaker σ-donating Br<sup>-</sup> vs. Cl<sup>-</sup> ligand in  $[(Ph_2phen)_2Ru(dpp)RhX_2(Ph_2phen)]^{3+}$  is proposed to more rapidly form the active Ru(II),Rh(I) species, as well as minimize the degree of ion pairing that impedes catalyst activity throughout the photocatalytic cycle. With regards to the weaker σ-donating dmeb ligand in **Ru-Rh(dmeb)**, more rapid Cl<sup>-</sup> dissociation upon photoexcitation generates the proposed  $[(Ph_2phen)_2Ru(dpp)Rh^I(dmeb)]^{3+}$  more efficiently to interact with H<sub>2</sub>O and evolve H<sub>2</sub>. The photocatalytic robustness of **Ru-Rh(dmeb)** is enhanced when compared with **Ru-Rh(Me<sub>2</sub>bpy)** and **Ru-Rh(bpy)**, which suggests the methyl-ester substituents inhibit catalyst deactivation until later times.

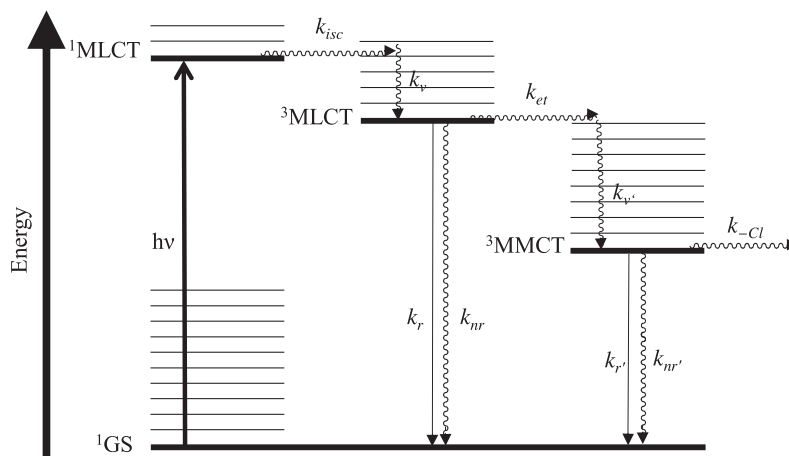


**Fig. 6.** Simplified Jablonski diagram depicting potential excited states and deactivation processes within the Ru(II),Rh(III) bimetallic architecture. GS = ground state, MLCT = metal-to-ligand charge transfer, MMCT = metal-to-metal charge transfer,  $k_{isc}$  = rate constant for intersystem crossing,  $k_v$  = rate constant for vibrational relaxation,  $k_r$  = rate constant for radiative decay,  $k_{nr}$  = rate constant for non-radiative decay,  $k_{et}$  = rate constant for intramolecular electron transfer,  $k_{-Cl}$  = rate constant for Cl<sup>-</sup> dissociation.

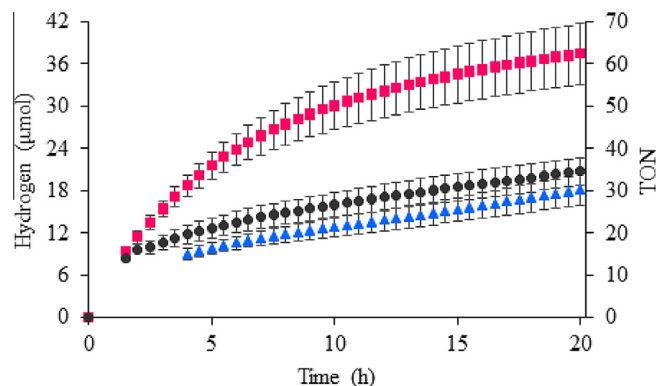


**Fig. 7.** Photocatalytic H<sub>2</sub> production and catalyst turnover numbers (TON) for **Ru-Rh(Me<sub>2</sub>bpy)** (triangles), **Ru-Rh(bpy)** (circles), and **Ru-Rh(dmeb)** (squares). Conditions:  $\lambda^{exc}$  = 470 nm, solvent = DMF, [photocatalyst] = 130 μM, [H<sub>2</sub>O] = 0.62 M, [DMA] = 1.5 M, [DMAH<sup>+</sup>][CF<sub>3</sub>SO<sub>3</sub><sup>-</sup>] = 110 μM.

**Table 3**  
Hydrogen evolution turnover numbers (TON) and maximum quantum yields for **Ru-Rh(Me<sub>2</sub>bpy)**, **Ru-Rh(bpy)** and **Ru-Rh(dmeb)**.

Complex	$k_{-Cl}$ (s <sup>-1</sup> )	TON <sup>a</sup>	Max. Φ
<b>Ru-Rh(Me<sub>2</sub>bpy)</b>	0.2	30 ± 4	0.002
<b>Ru-Rh(bpy)</b>	0.2	35 ± 3	0.003
<b>Ru-Rh(dmeb)</b>	0.7	63 ± 7	0.004

<sup>a</sup> Mole H<sub>2</sub> per mole catalyst after 20 h photolysis.

The rate constants for excited state intramolecular electron transfer (10<sup>7</sup> s<sup>-1</sup>) and deactivation (10<sup>3</sup>–10<sup>6</sup> s<sup>-1</sup>), as well as bimolecular quenching by a sacrificial electron donor (4.9 × 10<sup>9</sup> M<sup>-1</sup> s<sup>-1</sup> for  $[(bpy)_2Ru(dpp)RhCl_2(bpy)]^{3+}$  and DMA) [46], are several orders of magnitude greater than the electrochemically determined rate constants for chloride loss (10<sup>-1</sup> s<sup>-1</sup>). Intramolecular electron transfer to populate the <sup>3</sup>MMCT excited state and bimolecular quenching from DMA occur rapidly to create a state similar to the electrochemically reduced product,  $[(Ph_2phen)_2Ru^II(dpp)Rh^I Cl_2(R_2-bpy)]^{2+}$ . In this scenario, chloride dissociation represents a potential rate limiting step in water reduction catalysis and the weaker σ-donating methyl ester substituents on bpy facilitate more rapid chloride dissociation.

#### 4. Conclusions

The new Ru(II),Rh(III) bimetallic complexes **Ru-Rh(Me<sub>2</sub>bpy)**, **Ru-Rh(bpy)**, and **Ru-Rh(dmeb)** were synthesized and characterized to investigate the influence that Rh-TL variation has on the electrochemical, photophysical, and photocatalytic properties. Electrochemical data indicate a Ru-based HOMO and Rh-based LUMO for all three bimetallics. The bimetallic complexes are efficient light absorbers throughout the UV and visible with the lowest energy transition displaying Ru(dπ) → μ-dpp(π\*)<sup>1</sup>MLCT character. Photoexcitation results in population of a weakly-emissive, short-lived Ru(dπ) → μ-dpp(π\*)<sup>3</sup>MLCT excited state that undergoes intramolecular electron transfer to populate a non-emissive, photochemically-active Ru(dπ) → Rh(dσ\*)<sup>3</sup>MMCT excited state. The above properties are important requirements for the design of photocatalysts for H<sub>2</sub>O reduction *via* photoinitiated electron collection at a Rh metal center. The new bimetallic complexes are able to catalyze the reduction of H<sub>2</sub>O to H<sub>2</sub> in the presence of light and a sacrificial electron donor and the **Ru-Rh(dmeb)** complex displayed enhanced activity compared to the **Ru-Rh(Me<sub>2</sub>bpy)** and **Ru-Rh(bpy)** complexes. Although the photophysical properties of the three complexes did not vary greatly, the rate constant for chloride dissociation (*k*<sub>-Cl</sub>) was impacted and the weaker σ-donating –COOCH<sub>3</sub> substituted bipyridine TL possessed a larger *k*<sub>-Cl</sub> value (0.7 s<sup>-1</sup>) compared to the stronger σ-donating –CH<sub>3</sub> and –H substituted bipyridine TL (*k*<sub>-Cl</sub> = 0.2 s<sup>-1</sup>). Substitution with ester groups decreases the σ-donating ability of the bipyridine ligand, thereby stabilizing the Rh(dσ\*) orbitals and expediting cleavage of the Rh–Cl bond to form the active catalytic species.

#### Acknowledgements

Acknowledgement is made to the Chemical Sciences, Geosciences and Biosciences Division, Office of Basic Energy Sciences, Office of Sciences, U.S. Department of Energy (DE-FG02-05ER15751) for funding of this research. The authors would also like to thank Mr. William Bebout (Analytical Services, Department of Chemistry, Virginia Tech) and Mr. T.J. Rohrabough for assistance with ESI mass spectrometry and Prof. James M. Tanko (Department of Chemistry, Virginia Tech) for valuable discussions and helpful electrochemical insight. We thank Prof. Claudia Turro (Department of Chemistry and Biochemistry, The Ohio State University) for use of the time correlated single photon counter and insightful discussions.

#### References

- [1] A.J. Bard, M.A. Fox, Artificial photosynthesis – solar splitting of water to hydrogen and oxygen, *Acc. Chem. Res.* 28 (1995) 141–145.
- [2] N.S. Lewis, D.G. Nocera, Powering the planet: chemical challenges in solar energy utilization, *Proc. Natl. Acad. Sci. U.S.A.* 103 (2006) 15729–15735.
- [3] D.G. Nocera, The artificial leaf, *Acc. Chem. Res.* 45 (2012) 767–776.
- [4] M.G. Walter, E.L. Warren, J.R. McKone, S.W. Boettcher, Q. Mi, E.A. Santori, N.S. Lewis, Solar water splitting cells, *Chem. Rev.* 110 (2010) 6446–6473.
- [5] W.T. Eckenhoff, R. Eisenberg, Molecular systems for light driven hydrogen production, *Dalton Trans.* 41 (2012) 13004–13021.
- [6] S. Berardi, S. Drouet, L. Francas, C. Gimbert-Surinach, M. Guttentag, C. Richmond, T. Stoll, A. Llobet, Molecular artificial photosynthesis, *Chem. Soc. Rev.* 43 (2014) 7501–7519.
- [7] M. Kirch, J.M. Lehn, J.P. Sauvage, Hydrogen Generation by visible-light irradiation of aqueous-solutions of metal-complexes – approach to the photo-chemical conversion and storage of solar-energy, *Helv. Chim. Acta* 62 (1979) 1345–1384.
- [8] J.M. Lehn, J.P. Sauvage, Chemical storage of light energy – catalytic generation of hydrogen by visible-light or sunlight – irradiation of neutral aqueous-solutions, *Nouv. J. Chim.* 1 (1977) 449–451.
- [9] V. Balzani, L. Mogggi, F. Scandola, Towards a supramolecular photochemistry: assembly of molecular components to obtain photochemical molecular devices, in: V. Balzani (Ed.), *Supramolecular Photochemistry*, Springer, Netherlands, 1987, pp. 1–28.
- [10] S. Rau, B. Schäfer, D. Gleich, E. Anders, M. Rudolph, M. Friedrich, H. Görls, W. Henry, J.G. Vos, A supramolecular photocatalyst for the production of hydrogen and the selective hydrogenation of toluene, *Angew. Chem. Int. Ed.* 45 (2006) 6215–6218.
- [11] H. Ozawa, M.-A. Haga, K. Sakai, A photo-hydrogen-evolving molecular device driving visible-light-induced EDTA-reduction of water into molecular hydrogen, *J. Am. Chem. Soc.* 128 (2006) 4926–4927.
- [12] S.M. Molnar, G. Nallas, J.S. Bridgewater, K.J. Brewer, Photoinitiated electron collection in a mixed-metal trimetallic complex of the form ((Bpy)<sub>2</sub>Ru(dpb)(2)IrCl<sub>2</sub>)(PF<sub>6</sub>)<sub>5</sub> (bpy = 2,2'-Bipyridine and dpb = 2,3-bis(2-pyridyl)benzoquinoxaline), *J. Am. Chem. Soc.* 116 (1994) 5206–5210.
- [13] M.J. Kim, R. Konduri, H.W. Ye, F.M. MacDonnell, F. Puntoriero, S. Serroni, S. Campagna, T. Holder, G. Kinsel, K. Rajeshwar, Dinuclear ruthenium(II) polypyridyl complexes containing large, redox-active, aromatic bridging ligands: synthesis, characterization, and intramolecular quenching of MLCT excited states, *Inorg. Chem.* 41 (2002) 2471–2476.
- [14] R. Konduri, H.W. Ye, F.M. MacDonnell, S. Serroni, S. Campagna, K. Rajeshwar, Ruthenium photocatalysts capable of reversibly storing up to four electrons in a single acceptor ligand: a step closer to artificial photosynthesis, *Angew. Chem. Int. Ed.* 41 (2002) 3185.
- [15] M. Elvington, K.J. Brewer, Photoinitiated electron collection at a metal in a rhodium-centered mixed-metal supramolecular complex, *Inorg. Chem.* 45 (2006) 5242–5244.
- [16] M. Elvington, J. Brown, S.M. Arachchige, K.J. Brewer, Photocatalytic hydrogen production from water employing a Ru, Rh, Ru molecular device for photoinitiated electron collection, *J. Am. Chem. Soc.* 129 (2007) 10644–10645.
- [17] G.F. Manbeck, K.J. Brewer, Photoinitiated electron collection in polyazine chromophores coupled to water reduction catalysts for solar H<sub>2</sub> production, *Coord. Chem. Rev.* 257 (2013) 1660–1675.
- [18] M.G. Pfeffer, T. Kowacs, M. Waechtler, J. Guthmuller, B. Dietzek, J.G. Vos, S. Rau, Optimization of hydrogen-evolving photochemical molecular devices, *Angew. Chem. Int. Ed.* 54 (2015) 6627–6631.
- [19] T. Stoll, C.E. Castillo, M. Kayanuma, M. Sandroni, C. Daniel, F. Odobel, J. Fortage, M.-N. Collomb, Photo-induced redox catalysis for proton reduction to hydrogen with homogeneous molecular systems using rhodium-based catalysts, *Coord. Chem. Rev.* 304 (2015) 20–37.
- [20] J.K. White, K.J. Brewer, A new Ru, Ru, Pt supramolecular architecture for photocatalytic H<sub>2</sub> production, *Chem. Commun.* 51 (2015) 16123–16126.
- [21] Y. Halpin, M.T. Pryce, S. Rau, D. Dini, J.G. Vos, Recent progress in the development of bimetallic photocatalysts for hydrogen generation, *Dalton Trans.* 42 (2013) 16243–16254.
- [22] M. Schulz, M. Karnahl, M. Schwalbe, J.G. Vos, The role of the bridging ligand in photocatalytic supramolecular assemblies for the reduction of protons and carbon dioxide, *Coord. Chem. Rev.* 256 (2012) 1682–1705.
- [23] H. Ozawa, K. Sakai, Photo-hydrogen-evolving molecular devices driving visible-light-induced water reduction into molecular hydrogen: structure-activity relationship and reaction mechanism, *Chem. Commun.* 47 (2011) 2227–2242.
- [24] S.A. Arachchige, J. Brown, K.J. Brewer, Photochemical hydrogen production from water using the new photocatalyst [(bpy)<sub>2</sub>Ru(dpp)]<sub>2</sub>[RhBr<sub>2</sub>](PF<sub>6</sub>)<sub>5</sub>, *J. Photochem. Photobiol. A* 197 (2008) 13–17.
- [25] S.M. Arachchige, J.R. Brown, E. Chang, A. Jain, D.F. Zigler, K. Rangan, K.J. Brewer, Design considerations for a system for photocatalytic hydrogen production from water employing mixed-metal photochemical molecular devices for photoinitiated electron collection, *Inorg. Chem.* 48 (2009) 1989–2000.
- [26] H.M. Rogers, S.M. Arachchige, K.J. Brewer, Enhancement of solar fuel production schemes by using a Ru, Rh, Ru supramolecular photocatalyst containing hydroxide labile ligands, *Chem. Eur. J.* 21 (2015) 16948–16954.
- [27] T.A. White, S.L.H. Higgins, S.M. Arachchige, K.J. Brewer, Efficient photocatalytic hydrogen production in a single-component system using Ru, Rh, Ru supramolecules containing 4,7-diphenyl-1,10-phenanthroline, *Angew. Chem. Int. Ed.* 50 (2011) 12209–12213.
- [28] T.A. White, K. Rangan, K.J. Brewer, Synthesis, characterization, and study of the photophysical and photocatalytic properties of the photoinitiated electron collector [([phen]<sub>2</sub>Ru(dpp))<sub>2</sub>RhBr<sub>2</sub>](PF<sub>6</sub>)<sub>5</sub>, *J. Photochem. Photobiol. A* 209 (2010) 203–209.
- [29] D.F. Zigler, J. Wang, K.J. Brewer, Ruthenium(II)-polyazine light absorbers bridged to reactive cis-dichlororhodium(III) centers in a bimetallic molecular architecture, *Inorg. Chem.* 47 (2008) 11342–11350.
- [30] H.M. Rogers, T.A. White, B.N. Stone, S.M. Arachchige, K.J. Brewer, Nonchromophoric halide ligand variation in polyazine-bridged Ru(II), Rh(III) bimetallic supramolecules offering new insight into photocatalytic hydrogen production from water, *Inorg. Chem.* 54 (2015) 3545–3551.
- [31] J. Wang, T.A. White, S.M. Arachchige, K.J. Brewer, A new structural motif for photoinitiated electron collection: Ru, Rh bimetallics providing insight into H<sub>2</sub> production via photocatalysis of water reduction by Ru, Rh, Ru supramolecules, *Chem. Commun.* 47 (2011) 4451–4453.
- [32] T.A. White, H.E. Mallalieu, J. Wang, K.J. Brewer, Mechanistic insight into the electronic influences imposed by substituent variation in polyazine-bridged ruthenium(II)/rhodium(III) supramolecules, *Chem. Eur. J.* 20 (2014) 8265–8268.
- [33] T.A. White, B.N. Whitaker, K.J. Brewer, Discovering the balance of steric and electronic factors needed to provide a new structural motif for photocatalytic hydrogen production from water, *J. Am. Chem. Soc.* 133 (2011) 15332–15334.

- [34] R. Zhou, G.F. Manbeck, D.G. Wimer, K.J. Brewer, A new (RuRhIII)-Rh-II bimetallic with a single Rh-Cl bond as a supramolecular photocatalyst for proton reduction, *Chem. Commun.* 51 (2015) 12966–12969.
- [35] C.M. Bolinger, N. Story, B.P. Sullivan, T.J. Meyer, Electrocatalytic reduction of carbon-dioxide by 2,2'-bipyridine complexes of rhodium and iridium, *Inorg. Chem.* 27 (1988) 4582–4587.
- [36] S.C. Rasmussen, M.M. Richter, E. Yi, H. Place, K.J. Brewer, Synthesis and characterization of a series of novel rhodium and iridium complexes containing polypyridyl bridging ligands – potential uses in the development of multimetal catalysts for carbon-dioxide reduction, *Inorg. Chem.* 29 (1990) 3926–3932.
- [37] D.D. Perrin, *Dissociation Constants of Organic Bases in Aqueous Solution*, Butterworths Scientific Publications, London, 1965.
- [38] A.R. Oki, R.J. Morgan, An efficient preparation of 4, 4'-dicarboxy-2, 2'-bipyridine, *Synth. Commun.* 25 (1995) 4093–4097.
- [39] L.A. Basile, J.K. Barton, Design of a double-stranded DNA cleaving agent with two polyamine metal-binding arms: Ru(DIP)2Macron+, *J. Am. Chem. Soc.* 109 (1987) 7548–7550.
- [40] M.T. Mongelli, K.J. Brewer, Synthesis and study of the light absorbing, redox and photophysical properties of Ru(II) and Os(II) complexes of 4,7-diphenyl-1,10-phenanthroline containing the polyazine bridging ligand 2,3-bis(2-pyridyl)pyrazine, *Inorg. Chem. Commun.* 9 (2006) 877–881.
- [41] R. Bieda, I. Ott, M. Dobroschke, A. Prokop, R. Gust, W.S. Sheldrick, Structure-activity relationships and DNA binding properties of apoptosis inducing cytotoxic rhodium(III) polypyridyl complexes containing the cyclic thioether [9]aneS3, *J. Inorg. Biochem.* 103 (2009) 698–708.
- [42] M. Rudolph, D.P. Reddy, S.W. Feldberg, A simulator for cyclic voltammetric responses, *Anal. Chem.* 66 (1994) 589A–600A.
- [43] BASi DigiSim® Simulation Software for Cyclic Voltammetry.
- [44] J.R. Brown, M. Elvington, M.T. Mongelli, D.F. Zigler, K.J. Brewer, Analytical methods development for supramolecular design in solar hydrogen production, *SPIE Optics + Photonics* 6340 (2006) 634017.
- [45] A.J. Bard, L.R. Faulkner, *Electrochemical Methods: Fundamentals and Applications*, 2nd ed., John Wiley & Sons Inc., Hoboken, NJ, 2001.
- [46] A.T. Wagner, R. Zhou, K.S. Quinn, T.A. White, J. Wang, K.J. Brewer, Tuning the photophysical properties of Ru(II) monometallic and Ru(II), Rh(III) bimetallic supramolecular complexes by selective ligand deuteration, *J. Phys. Chem. A* 119 (2015) 6781–6790.
- [47] M. Elvington, K.J. Brewer, Photoinitiated electron collection at a metal in a rhodium-centered mixed-metal supramolecular complex, *Inorg. Chem.* 45 (2006) 5242–5244.
- [48] T.A. White, S.M. Arachchige, B. Sedai, K.J. Brewer, Emission spectroscopy as a probe into photoinduced intramolecular electron transfer in polyazine bridged Ru(II), Rh(III) supramolecular complexes, *Materials* 3 (2010) 4328–4354.